Draft version June 1, 2023
Typeset using LaTeX **twocolumn** style in AASTeX631

Speckle Interferometry at SOAR in 2022

Brian D. Mason,[1] Andrei Tokovinin,[2] Rene A. Mendez,[3] and Edgardo Costa[3]

[1] *U.S. Naval Observatory, 3450 Massachusetts Ave., Washington, DC, USA*
[2] *Cerro Tololo Inter-American Observatory — NFSs NOIRLab Casilla 603, La Serena, Chile*
[3] *Universidad de Chile, Casilla 36-D, Santiago, Chile*

ABSTRACT

Results of the speckle-interferometry observations at the 4.1 m SOuthern Astrophysical Research Telescope (SOAR) obtained during 2022 are presented: 2507 measurements of 1925 resolved pairs or subsystems and 787 non-resolutions of 613 targets; 26 pairs are resolved here for the first time. This work continues our long-term effort to monitor orbital motion in close binaries and hierarchical systems. A large number of orbits have been updated using these measurements.

Keywords: binaries:visual

1. INTRODUCTION

This paper continues the series of double-star measurements made at the 4.1 m SOuthern Astrophysical Research Telescope (SOAR) since 2008 with the speckle camera, HRCam. Previous results are published by Tokovinin, Mason, & Hartkopf (2010a, hereafter TMH10) and in (Tokovinin et al. 2010b; Hartkopf et al. 2012; Tokovinin 2012; Tokovinin et al. 2014, 2015, 2016, 2018a, 2019, 2020, 2021, 2022). Observations reported here were made during 2022.

The structure and content of this paper are similar to other paper of this project. Section 2 reviews all speckle programs that contributed to this paper, the observing procedureand the data reduction. The results are presented in Section 3 in the form of electronic tables archived by the journal. We also discuss new resolutions and present orbits resulting from this data set. A short summary and an outlook of further work in Section 4 close the paper.

2. OBSERVATIONS

2.1. *Observing Programs*

As in previous years, HRCam (see § 2.2) was used during 2022 to execute several observing programs, some with common targets. Table 1 gives an overview of these programs and indicates which observations are published in the present paper. The numbers of observations are approximate. Here is a brief description of the main programs.

Orbits of resolved binaries: New measurements contribute to the steady improvement of the quantity and quality of orbits in the Sixth Catalog of Orbits of Visual Binary Stars (Hartkopf, Mason & Worley 2001). See Anguita-Aguero et al. (2022); Gómez et al. (2022) as recent examples of this work. We provide large tables of reliable and preliminary orbits in §3.3.

Hierarchical systems of stars are of special interest because their architecture is relevant to star formation; dynamical evolution of these hierarchies increases chances of stellar interactions and mergers (Tokovinin 2021b). Orbital motions of several triple systems are monitored at SOAR and these data are used for the orbit determinations (Tokovinin & Latham 2020; Tokovinin 2021a, 2023a).

Hipparcos binaries within 200 pc are monitored to measure masses of stars and to test stellar evolutionary models, as outlined by, e.g., Horch et al. (2015, 2017, 2019). The southern part of this sample is addressed at SOAR (Mendez et al. 2017). This program overlaps with the general work on visual orbits.

brian.d.mason.civ@us.navy.mil
andrei.tokovinin@noirlab.edu
rmendez@uchile.cl

Table 1. Observing programs

Program	PI	N	Publ.[a]
Orbits, hierarchies	Mason, Tokovinin	1402	Yes
Hipparcos binaries	Mendez, Costa	247	Yes
Neglected binaries	R. Gould, Mason	390	Yes
Nearby M dwarfs	E. Vrijmoet	323	Some
TESS follow-up	C. Ziegler	739	No
Acceleration stars	K. Franson	188	No
Gaia hierarchies	Tokovinin	1203	No
Wide pairs	J. Chanamé	275	No

[a] This columns indicates whether the results are published here (Yes), published partially (Some), or deferred to future papers (No).

Neglected close binaries from the Washington Double Star Catalog, WDS (Mason et al. 2001),[1] were observed as a "filler" at low priority. In some cases, we resolved new inner subsystems, thus converting classical visual pairs into hierarchical triples. In other cases we identified neglected pairs as spurious doubles in §3.4.

Nearby M dwarfs are being observed at SOAR since 2018 following the initiative of T. Henry and E. Vrijmoet. The goal is to assemble statistical data on orbital elements, focusing on short periods. First results on M dwarfs are published by Vrijmoet et al. (2022). In 2022, we continued to monitor these pairs; a paper on their orbits is in preparation. Measurements of previously known pairs are published here, those of newly resolved pairs are deferred to the paper in preparation.

TESS follow-up continues the program executed in 2018–2020. Its results are published in (Ziegler et al. 2020, 2021). All speckle observations of TESS targets of interest are promptly posted on the EXOFOP web site. These data are used in the growing number of papers on TESS exoplanets, mostly as limits on close companions to exohosts.

Acceleration stars were observed as potential targets of high-contrast imaging of exoplanets in a program led by K. Franson and B. Bowler (continued from 2021).

Gaia candidate hierarchies are wide binaries in the 100-pc catalog where one or both components have indications of unresolved subsystems in the Gaia data. A thousand of these candidates were observed during 2021–2023, about half were resolved, as reported in Tokovinin (2023b).

Wide pairs were observed for the program led by J. Chanamé.

[1] See the latest online WDS version.

If observations of a given star were requested by several programs, they are published here even when the other program still continues. We also publish here the measurements of previously known pairs resolved during surveys, for example in the TESS follow-up.

Speckle observations in 2022 were conducted during 13 observing runs for a total of approximately 18 nights (14 nights allocated and four nights of engineering time, usually second halves). A total of 5974 observations (including calibrators and refererence stars) were made, 332 targets per night on average.

2.2. *Instrument and Observing Procedure*

The observations reported here were obtained with the *high-resolution camera* (HRCam) — a fast imager designed to work at the 4.1 m SOAR telescope (Tokovinin 2018). The instrument and observing procedure are described in the previous papers of these series (e.g. Tokovinin et al. 2020), so only the basic facts are restated here. HRCam receives light through the SOAR Adaptive Module (SAM) which provides correction of the atmospheric dispersion. We used mostly the near-infrared I filter (824±170 nm) and the Strömgren y filter (543±22 nm); the transmission curves of HRCam filters are given in the instrument manual. In the standard observing mode, two series of 400 200×200 pixel images (image cubes) are recorded. The pixel scale is $0\farcs01575$, so the field of view is $3\farcs15$; the exposure time is normally 24 ms. For survey programs such as TESS follow-up, we use the I filter and a 2×2 binning, doubling the field. Pairs wider than $\sim1\farcs4$ are observed with a 400×400 pixel fieldand the widest pairs are sometimes recorded with the full field of 1024 pixels (16″) and a 2×2 binning.

The speckle power spectra are calculated and displayed immediately after the acquisition for quick evaluation of the results. Observations of close pairs are accompanied by observations of single stars for reference to account for such instrumental effects as telescope vibration or aberrations. Bright stars can be resolved and measured below the formal diffraction limit by fitting a model to the power spectrum and using the reference. The resolution and contrast limits of HRCam are further discussed in TMH10 and in the previous papers of this series. The standard magnitude limit is $I \approx 12$ mag under typical seeing; pairs as faint as $I \approx 16$ mag have been measured under exceptionally good seeing, albeit with reduced accuracy and resolution.

Custom software helps to optimize observations by selecting targets, pointing the telescope and logging. The observing programs are executed in an optimized way, depending on the target visibility, atmospheric conditionsand priorities, while minimizing the telescope slews. Reference stars and calibrator binaries are observed alongside the main targets as needed; their observations are published here as well.

Table 2. Measurements of Double Stars at SOAR

Col.	Label	Format	Description, units
1	WDS	A10	WDS code (J2000)
2	Discov.	A16	Discoverer code
3	Other	A12	Alternative name
4	RA	F8.4	R.A. J2000 (deg)
5	Dec	F8.4	Declination J2000 (deg)
6	Epoch	F9.4	Julian year (yr)
7	Filt.	A2	Filter
8	N	I2	Number of averaged cubes
9	θ	F8.1	Position angle (deg)
10	$\rho\sigma_\theta$	F5.1	Tangential error (mas)
11	ρ	F8.4	Separation (arcsec)
12	σ_ρ	F5.1	Radial error (mas)
13	Δm	F7.1	Magnitude difference (mag)
14	Flag	A1	Flag of magnitude difference[a]
15	$(\mathrm{O-C})_\theta$	F8.1	Residual in angle (deg)
16	$(\mathrm{O-C})_\rho$	F8.3	Residual in separation (arcsec)
17	Ref	A9	Orbit reference[b]

[a] Flags: q – the quadrant is determined; * – Δm and quadrant from average image; : – noisy data or tentative measures.

[b] References are provided at https://crf.usno.navy.mil/data_products/WDS/orb6/wdsref.html

2.3. *Data Processing*

The data processing is described in TMH10 and Tokovinin (2018). We use the standard speckle interferometry technique based on the calculation of the power spectrum and the speckle auto-correlation function (ACF). Companions are detected as secondary peaks in the ACF and/or as fringes in the power spectrum. Parameters of the binary and triple stars: separation (ρ), position angle (θ), and magnitude difference (Δm) are determined by modeling (fitting) the observed power spectrum. The true quadrant is found from the shift-and-add (SAA) images whenever possible because the standard speckle interferometry determines position angles modulo 180°. The resolution and detection limits are estimated for each observation.

Calibration of pixel scale and orientation is based on a set of wide pairs with well-modeled motion. The system of calibrators is tied to Gaia astrometry. Further details can be found in Tokovinin et al. (2022).

3. RESULTS

3.1. *Data Tables*

The results (measures of resolved pairs and non-resolutions) are presented in exactly the same format as in Tokovinin et al. (2021, 2022). The long tables are published electronically; here we describe their content.

Table 2 lists 2507 measures of 1925 resolved pairs and subsystems, including new discoveries. The pairs are identified by their WDS-style codes based on the J2000 coordinates and discoverer designations adopted in the WDS catalog (Mason et al. 2001), as well as by alternative names in column (3), mostly from the Hipparcos catalog. Equatorial coordinates for the epoch J2000 in degrees are given in columns (4) and (5) to facilitate matching with other catalogs and databases. Circumstances of this particular observation (JY, filter, number of cubes), be it Table 1 or 2, are given in columns (6) through (8). In the case of resolved multiple systems, the positional measurements and their errors (columns 9–12) and magnitude differences (column 13) refer to the individual pairings between components, not to their photocenters. As in the previous papers of this series, we list the internal errors derived from the power spectrum model and from the difference between the measures obtained from two data cubes. The real errors are usually larger, especially for difficult pairs with substantial Δm and/or with small separations. Residuals from orbits and from the models of calibrator binaries, typically between 1 and 5 mas rms, characterize the external errors of the HRCam astrometry.

The flags in column (14) indicate the cases where the true quadrant is determined (otherwise the position angle is measured modulo 180°), when the relative photometry of wide pairs is derived from the long-exposure images (this reduces the bias caused by speckle anisoplanatism), and when the data are noisy or the resolutions are tentative (see TMH10). For binary stars with known orbits, the residuals to the latest orbit and its reference are provided in columns (15)–(17). Residuals close to 180° mean that the orbit swaps the brighter (A) and fainter (B) stars. However, in some binaries the secondary is fainter in one filter and brighter in the other (e.g. WDS15234−5919). In these cases, it is better to keep the historical identification of the components in agreement with the orbit and to provide a negative magnitude difference Δm.

The 787 non-resolutions of 613 systems are reported in Table 3. Its first columns (1) to (8) have the same meaning and format as in Table 2. Column (9) gives the minimum resolvable separation when pairs with $\Delta m < 1$ mag are detectable. It is computed from the maximum spatial frequency of the useful signal in the power spectrum and is normally close to the formal diffraction limit

Table 3. Unresolved Stars

Col.	Label	Format	Description, units
1	WDS	A10	WDS code (J2000)
2	Discov.	A16	Discoverer code
3	Other	A12	Alternative name
4	RA	F8.4	R.A. J2000 (deg)
5	Dec	F8.4	Declination J2000 (deg)
6	Epoch	F9.4	Julian year (yr)
7	Filt.	A2	Filter
8	N	I2	Number of averaged cubes
9	$\rho_{\rm min}$	F7.3	Angular resolution (arcsec)
10	$\Delta m(0.15)$	F7.2	Max. Δm at $0\farcs15$ (mag)
11	$\Delta m(1)$	F7.2	Max. Δm at $1''$(mag)
12	Flag	A1	: marks noisy data

($\frac{\lambda}{D}$). The following columns (10) and (11) provide the indicative dynamic range, i.e., the maximum magnitude difference at separations of $0\farcs15$ and $1''$, respectively, at 5σ detection level. The last column (12) marks noisy data by the flag ":".

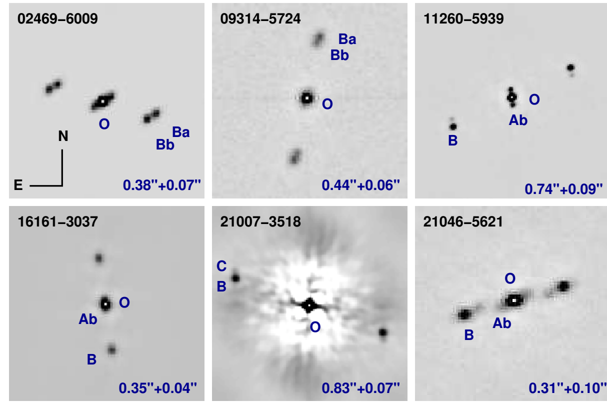

Figure 1. Fragments of speckle ACFs of six newly resolved triple stars. The spatial and intensity scale is chosen for best representation of each system. Blue letters mark the ACF peaks corresponding to the components' location, O marks the ACF center. The outer and inner separations are indicated.

3.2. *New Pairs*

Table 4. New Double Stars

WDS J2000	Name	ρ (arcsec)	Δm (mag)	Program[a]
01079-4519	HIP 5305	0.04	0.0	HIP[b]
01536-7018	HIP 8834	0.29	1.6	HIP[b]
01575-5212	RST 43Aa,Ab	0.08	1.4	MSC[c,d]
02469-6009	I 268Ba,Bb	0.07	0.0	NEG[c,d]
05090+0654	HIP 23961	1.84	2.0	HIP[d]
09275-7330	I 832Aa,Ab	0.05	1.3	NEG[c]
09314-5724	RST3644Ba,Bb	0.06	0.4	NEG[c,d]
11093-1141	HIP 54523	0.59	4.9	REF[d]
11260-5939	RST4476Aa,Ab	0.09	1.4	NEG[c,d]
11349-4908	HIP 56497	1.14	5.7	REF[d]
12241+0357	LDS4205Ba,Bb	0.07	0.0	MSC
13133-0756	HDS1851Ba,Bb	0.04	0.5	NEG[c,d]
13557-3117	HIP 68021	0.07	2.5	REF[d]
15531-1634	HDS2237Aa,Ab	0.04	1.4	NEG[c,d]
16000-2025	HLD 125CD	0.41	0.0	MSC[d]
16161-3037	I 1586Aa,Ab	0.04	1.6	ORB[d]
16580+0547	HD 153252	0.37	1.0	MSC[d]
17323-4828	HIP 85831	3.00	5.6	HIP[d]
17435-6856	HIP 86741	0.44	2.8	HIP[b]
18274-3007	HIP 90450	0.06	0.6	HIP[b,d]
20081-6745	HIP 99174	0.12	0.7	HIP[b]
20372-6234	HIP 101731	0.68	3.3	HIP[b]
20374-3444	HIP 101752	0.05	0.3	HIP[b]
20581-1510	HIP 103491	0.09	0.0	HIP[b]
21007-3518	BU 765BC	0.07	2.4	NEG[c,d]

Table 4 *continued*

Table 4 *(continued)*

WDS J2000	Name	ρ (arcsec)	Δm (mag)	Program[a]
21046-5621	RST1081Aa,Ab	0.10	1.6	NEG[c,d]
21077-4523	HIP 104296	0.03	0.0	HIP[b]
21232-1035	HIP 105589	0.68	3.1	HIP[b]
23435-5947	HIP 117033	0.24	2.4	HIP[b]

[a] HIP – Hipparcos suspected binary; MSC – multiple system; REF – reference star; NEG – neglected pair; ORB – orbit pair.

[b] Suspected binary in Gaia DR3.

[c] New subsystem in a neglected binary.

[d] See comments in the text.

Table 4 highlights the 26 pairs resolved for the first time in 2022. All measurements of these pairs are found in Table 2. The pairs are identified by the WDS-style codes and the discovery codes or other names. The following columns contain the separation ρ, the magnitude difference Δm, and the observing program. About half of the new resolutions are Hipparcos stars within 200 pc with an increased Reduced Unit Weight Error (RUWE) in Gaia DR3 (GDR3; Gaia collaboration 2021). The second largest group are subsystems discovered in previously neglected visual binaries that lacked recent measures; six new triples are illustrated in Figure 1. Comments on some systems follow.

01575−5212. The newly resolved pair RST 43 Aa,Ab belongs to a quadruple system where the 0.″4 pair RST 43BC is located at 3.″3 from star A, a G6/K1III+F giant. The outer pair is COO 10 AB. The resolution of A is supported by its large RUWE=20.2 in GDR3.

02469−6009 is a quadruple system where the new 0.″07 subsystem Ba,Bb has been discovered serendipitously in the 0.″4 visual pair I 268 AB. It has been observed at SOAR in 2016.96 without resolving the subsystem, owing to the lower quality of the power spectrum, while in 2022 the triple nature is clear (Figure 1). The outer component C of this system, at 20.″9, has common proper motion (PM) and parallax.

05090+0654. The newly resolved companion to HIP 23961 at 1.″84 is also found in GDR3 at a similar position of 144.°16 and 1.″8250. Both stars have accurate and matching parallaxes of 13.4 mas and matching PMs, while $\Delta G = 2.36$ mag. However, between 2016.0 and 2022.2 the relative position has changed by 95 mas, which corresponds to a PM difference of 15 mas yr^{-1}. Meanwhile, Gaia measured a relative PM of only 2.1 mas yr^{-1}. Future observations will help to settle this discrepancy.

09314−5724 is another triple system discovered by resolving the secondary component of the neglected 0.″4 visual pair RST3644 with only three measures in the WDS. The resolution (Figure 1) is confirmed in 2023.

11093−1141. A new faint 0.″6 companion to the K5/M0III giant HIP 54523 (HD 96906), observed as a point-source reference, was resolved only in filter y and unresolved in I, where the magnitude difference should be larger because the main star is very red.

11260−5939. The neglected 0.″7 pair RST 4476 contains a 0.″1 subsystem Aa,Ab (Figure 1). Very little information on this A2/2III star is available. Photometry suggests a distance of ∼500 pcand no motion in the outer pair is detected since its discovery in 1939.

11349−4908. The new faint companion at 1.″14 from the bright reference star HIP 56497 with a fast PM of 250 mas yr^{-1} could be optical.

13133−0756. The secondary star in the 0.″4 Hipparcos pair HDS 1851 was resolved at a separation of 0.″04, slightly below the diffraction limit, so only elongation is seen. However, the discovery has been confirmed in 2023. The estimated period of Ba,Bb is about 25 yr.

13557−3117. A close 0.″07 companion to the reference star HIP 68021 (HD 121397, G6/8III) was discovered unexpectedly. However, it could have been suspected by the large RUWE of 3.8 in GDR3 and by the acceleration reported by Brandt (2021).

15531−1634. Resolution of a 0.″04 subsystem Aa,Ab in the neglected Hipparcos binary HDS 2237 (HD 142074, F6/7V) is tentative; in 2023.3 it was not detected, although the quality of the power spectrum was worse than in 2022.3. Reality of the subsystem is supported indirectly by the large RUWE of 15.9 in GDR3 and by the PM acceleration (Brandt 2021), which is unlilkely to be produced by the outer 0.″4 pair A,B with an estimated period of ∼300 yr.

16000−2025. This system, previously known as a visual triple HLD 125 (AB at 2.″9 and AC at 27.″3), is converted into a quadruple by resolving star C into a 0.″4 equal pair. Star C was also seen double by Gaia: the DR3 catalog contains two nearly equal ($\Delta G = 0.10$ mag) sources at 0.″374 and 233.°0 relative position. Our observation was prompted by Gaia, which should be credited for this discovery.

16161−3037. The visual pair I 1568 was monitored by HRCam since 2008 to follow its slow orbit with $P =$ 160 yr. Unexpectedly, the 0.″04 pair Aa,Ab was detected in 2022.44 and confirmed in 2023. Re-examination of the HRCam data shows that Aa,Ab was also resolved in 2018.23, but overlooked at the time, and partially resolved in 2022.68. Estimated period of Aa,Ab is 10 yr; it is responsible for the large astrometric noise in

GDR3 (RUWE of 3.8). A wobble in the motion of AB caused by the subsystem could be detectable.

16580+0547 is a quaruple system HD 153252 (spectral type G0) of 3+1 hierarchy. The outer 60″ pair is CRV 942and its component A is a 5.52 day single-lined spectroscopic binary. Large astrometric noise of star A in GDR3 (RUWE of 8.6) suggested an intermediate subsystem Aa,Ab, which was indeed resolved at 0.″37. Its estimated period of ∼400 yr implies only a slow motion, so the large RUWE could be produced by the companion's light, rather than by the photocenter motion.

17323−4828. The faint companion found at 3″ from the high-PM star HIP 85831 is definitely optical. It is seen by Gaia DR3 at 1.″768 and 40.°2 with $\Delta G = 4.9$ mag and a parallax of −0.06 mas.

18274−3007. Star HIP 90450 with a large RUWE of 5.0 has been resolved at 0.″06. A short period is expectedand subsequent observations in 2022 and 2023 confirmed rapid retrograde motion of the new pair.

21007−3518. A new 0.″07 subsystem BC was resolved in a neglected 0.″7 visual binary BU 765 (Figure 1). The estimated period of BC, ∼10 yr, suggests rapid orbital motion.

21046−5621. A 0.″3 neglected pair RST 1981 turns into a spectacular triple with inner 0.″1 pair Aa,Ab (Figure 1).

3.3. *New and Updated Orbits*

With one exception described below, the orbits here computed were determined with the venerable `orbgrid` code described in Hartkopf, McAlister & Franz (1989). In this technique, an adaptive "three dimensional" grid search is performed for initial guesses of period P, epoch $T$and eccentricity e. Prior calculations of orbits for these pairs, as cited in Tables 5 & 6, provide good inital guesses of these elements. As the residuals are minimized, the grid spacing is reduced and this method continues until the grid steps fall below 0.01 yr in P and T and 0.001 in e. Measures with overly large residuals are given either lower or zero weightand the process repeats until the grid steps of 1% in magnitude of the prior iteration.

Individual measures are weighted according to the methodology described in §2.1 of Hartkopf, Mason & Worley (2001). This determines the weight of each observation based on N, the number of nights (often one) in a mean position, the observation technique, and a factor which takes into account the measured separation and the resolution capability of the telescope used for the observation.

A numerical "grade" is given to each calculated orbit. The subjective qualification of these numerical grades are: 1 = definitive, 2 = good, 3 = reliable, 4 = preliminary and 5 = indeterminate. The actual grading is done with an objective rubric evaluating each orbit by several criteria:

1. weighted rms residual in separation ($d\rho$);
2. weighted rms residual in relative separation ($\frac{d\rho}{\rho}$);
3. position angle (θ) coverage (most helpful evaluating high eccentricity orbits);
4. maximum gap in position angle coverage (θ);
5. phase coverage, calculated from P and T (most helpful evaluating high inclination orbits);
6. maximum gap in phase;
7. number of revolutions; and
8. total number of observations.

The final list of computed orbits are divided into two groups, reliable and preliminary. However, rather than basing this solely on the grade, the criteria is based on the criteria of Aitken (1964):

> "In general, it is not worth while to compute the orbit of a double star until the observed arc not only exceeds 180 degrees, but also defines both ends of the apparent ellipse."

The orbits meeting this criteria and having small ($\frac{\Delta P}{P}$) relative error are found in the table of reliable orbits and other orbit solutions are in the table of preliminary orbits. While these preliminary orbits may lack sufficient coverage at this time, they should allow the determination of accurate predicted positions for the next years. Some of these orbits were improved with the addition of data taken in the first half of 2023 which will be presented with the rest of the SOAR 2023 data next year.

In these tables, the system is identified by the WDS J2000 code and the Discoverer Designation, followed by the seven Campbell Elements. Following this, a reference to the most current Hartkopf, Mason & Worley (2001) orbit which has been here improved is given. This is followed by the orbit grade and a flag indicating if there is a note. In Table 5, the following line provides the error of each orbital element. The quoted precision of each element is determined from the precision of the error, which is given to two significant digits. In Table 6, errors are not provided, but the elements are given to the nearest degree for i, Ω and ω, to nearest tenth of a year for P and T and the to a tenth of a percent for a and e. If a higher precision is provided in Table 6, this is due to the precision of the error in that element.

Notes to individual systems in both tables follow.

3.3.1. *Notes to Individual Orbital Systems*

01388−1758 = LDS 838 : Using the parallax from GDR3 and the mass ratio from Worley & Behall (1973), individual masses of $\mathcal{M}_a$ = 0.1191±0.0018 $\mathcal{M}_\odot$ and $\mathcal{M}_b$ = 0.1144±0.0017 $\mathcal{M}_\odot$ are determined for these components. See Figure 2.

10112−3245 = HDS1469 : Radically different solution for this pair. See Figure 2.

13535+1257 = BEU 18 : This pair lacks data in the south to define that portion of the orbit. Data in Autumn 2023 or Spring 2031 whould characterize those parts of the orbit.

14516−4335 = FIN 319 : This pair lacks data when the secondary is east of the primary. However, the separation predicted here (0.″017) would be a challenge. Close to this may be the best we can do. It is predicted to move from 343.°0 & 0.″042 on 2031.0 counterclockwise to 214.°4 & 0.″047 on 2032.0. Observing the pair many times in 2031 will be key to improving this orbit.

15440+0231 = RDR 6Ba,Bb : Predicted to get as close as 0.″007 at periastron, observing "both ends of the apparent ellipse" will be challenging. However, measures approaching and coming out of periastron as well as non-detection (cf. Table 3) when predicted should adequately probe this in Autumn 2025.

15462−2804 = KOH 49Ca,Cb : This pair just needs more data to adequately define the eastern end of the apparent ellipse. It should get to widest separation by mid 2027 and begin closing at that time.

16555−0820 = KUI 75AB : Using parallax from van Leeuwen (2007) and the mass ratio from Harris et al. (1963), individual masses of $\mathcal{M}_a$ = 0.487±0.054 $\mathcal{M}_\odot$ and $\mathcal{M}_b$ = 0.487±0.054 $\mathcal{M}_\odot$ are determined for these components. See Figure 2.

17190−3459 = MLO 4AB : Using parallax from van Leeuwen (2007) and the mass ratio from Harris et al. (1963), individual masses of $\mathcal{M}_a$ = 0.65±0.12 $\mathcal{M}_\odot$ and $\mathcal{M}_b$ = 0.448±0.085 $\mathcal{M}_\odot$ are determined for these components. See Figure 2.

17304−0104 = STF2173AB : The program `orbgrid` was used here to identify measures having overly large residuals which were omitted from the solution. High-angular resolution measures only (speckle interferometry, adaptive optics, Hipparcos, phase grating interferometer) were coupled with radial velocities from Batten et al. (1991) and Duquennoy et al. (1991), to arrive at a combined solution using the `orbit` IDL code Tokovinin (2016c), resulting in additional orbital elements of $K_1 = 4.88 \pm 0.11$ km s^{-1}, $K_2 = 5.49 \pm 0.11$ km s^{-1}, $\gamma = -77.018 \pm 0.064$ km s^{-1}, and individual masses of $\mathcal{M}_a$ = 1.028±0.050 $\mathcal{M}_\odot$ and $\mathcal{M}_b$ = 0.914±0.046 $\mathcal{M}_\odot$ are determined for these components. In addition, an orbital parallax of 59.90±2.97 mas is determined, which compares quite well with the mean trigonometric parallax of 59.6071 mas from the Gaia collaboration (2018). See Figure 2.

3.4. *Spurious Pairs*

False detections of double stars can be caused by errors in pointing, in data processing, or by other reasons; cf. Table 5 and §4 of McAlister et al. (1993). Optical artefacts resembling binary companions are discussed in (Tokovinin, Mason, & Hartkopf 2010a; Tokovinin 2018). Identifying these spurious pairs will save observing time in the future by eliminating the need to followup and examine these targets. In Table 8 are listed pairs we consider as likely spurious. The table contains the WDS code and Discoverer designation, the method (Vis — visual micrometer, Sp — speckle, HIP — Hipparcos) and date of the original discovery and the year(s) it has been unresolved in this program. Following that is a code giving other indications supporting the characterization of the double as "spurious". These codes are: R — normal RUWE parameter in GDR3, hence lack of astrometric noise; L — long estimated period, making it unlikely that the pair has moved significantly between discovery epoch and 2022; S — short estimated period covered by non-resolutions; B — no PM anomaly in (Brandt 2021); V – artefact caused by telescope vibration. Likely orbital periods P^* are estimated from separation ρ and parallax ϖ as $P^* = (\rho/\varpi)^{3/2} M^{1/2}$, assimung a mass sum of $M = 2\mathcal{M}_\odot$. In the WDS (Mason et al. 2001), these pairs are not removed but are given an X code identifying them as a "dubious double" or a "bogus binary".

Table 8. Likely Spurious Pairs

WDS	Discoverer	Resolved	Unresolved[a]
00547−2227	B 14	0.″1 Vis 1926	2017−19, R
00558−1832	B 645	0.″2 Vis 1926	2008−23, R, L, B
01144−0755	WSI 70Aa,Ab	0.″2 Sp 2008	2012−21, R, B, V
01380+0946	TOK 688	0.″1 Sp 2015	2016−21, R, B, V
01487−3839	I 1610AB	0.″3 Vis 1927	2016−22, R, B
04381−1749	B 1939	0.″1 Vis 1932	2017−20, R, B
05250−0249	BAG 42Aa,Ab	0.″2 Sp 2009	2017−18, R
07074−2127	YSC 195	0.″05 Sp 2010	2016−18, R
07346−3336	B 1551	0.″2 Vis 1929	2018−19, R, V
08095−4720	WSI 55Ba,Bb	0.″1 Sp 2006	2009−2018, V
08246−0109	B 527AB	0.″2 Vis 1938	2010−21, R, S
08246−0345	CHR 172Aa,Ab	0.″2 Sp 1988	2011−21, R, S, V
10123−3124	WSI 128	1.″1 Sp 2010	2015−22, R
11006+0337	CHR 33	0.″2 Sp 1983	2014−17, R, B, L

Table 8 *continued*

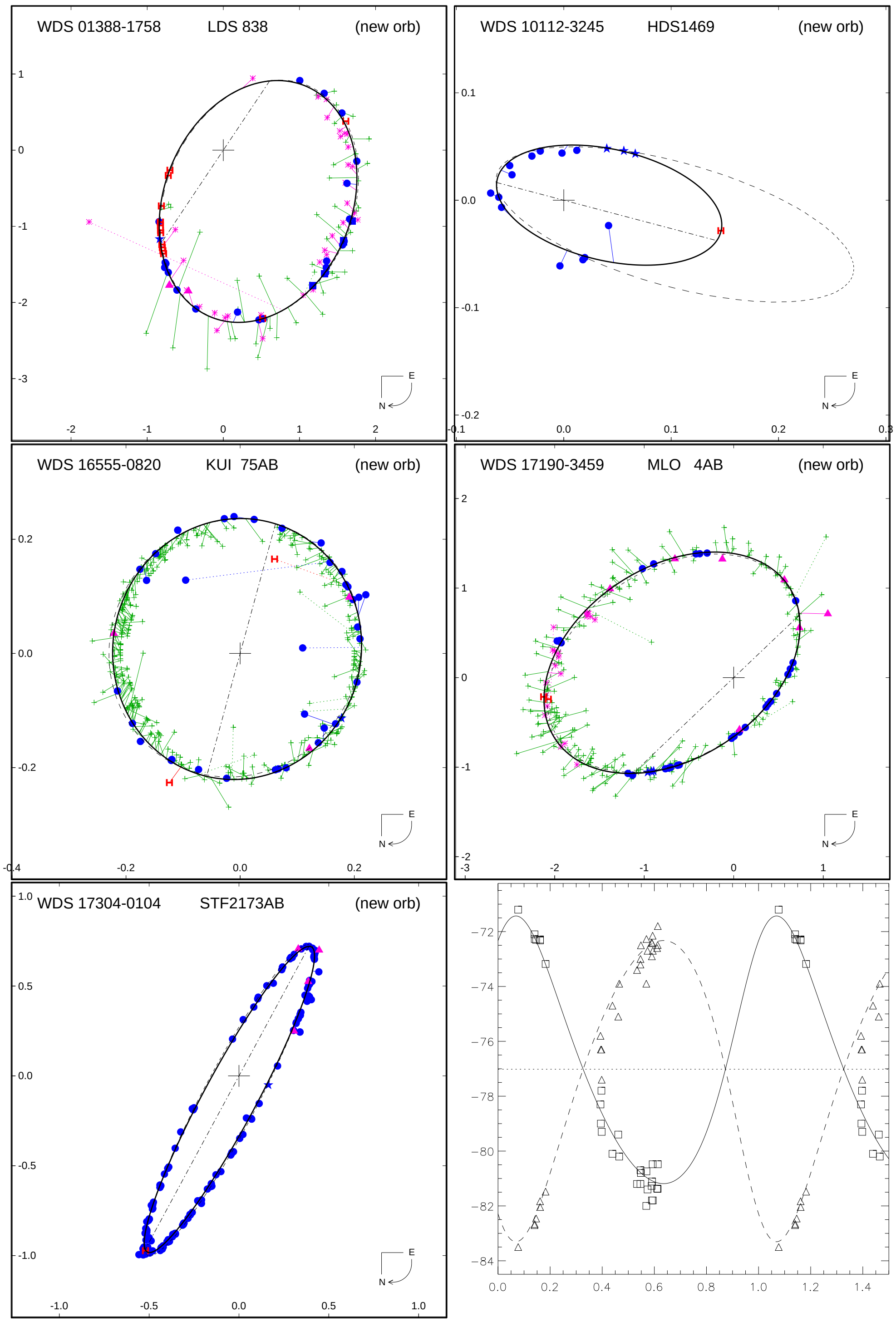

Figure 2. Selected new orbital solutions, plotted together with all published data in the WDS database as well as the new data in Table 2. In each of these figures, micrometric observations are indicated by plus signs, interferometric measures by filled circles, conventional CCD by pink triangles, space-based measures are indicated by the letter 'H', new measures from Table 2 are plotted as a filled star. "$O-C$" lines connect each measure to its predicted position along the new orbit (shown as a thick solid line). A dot-dash line indicates the line of nodesand a curved arrow in the lower right corner of each figure indicates the direction of orbital motion. The earlier orbit referenced in Table 5 is shown as a dashed ellipse. For the combined orbit of 17304−0104 = STF2173, plots of the relative astrometry and the radial velocity curve are provided.

Table 8 *(continued)*

WDS	Discoverer	Resolved	Unresolved[a]
11042−5828	HLN 22Aa,Ab	0.″2 Vis 1967	2009, R, L
11317+1422	WSI 101Aa,Ab	0.″1 Sp 2001	2011−18, R, S
11479+0815	CHR 134Aa,Ab	0.″3 Sp 1987	2014−17, R
11518−0546	CHR 36	0.″2 Sp 1983	2014, R, L
11545−5325	YMG 39	0.″03 Sp 2019	2019−21, R, S
12062−2002	B 1714	0.″1 Vis 1929	2018−22, R, B
12532−0333	CHR 38	0.″5 Sp 1984	2013−19, R, B
12543−1139	CHR 206	0.″04 Sp 1984	2014−17, R, S
13208−1127	HDS1872	0.″1 HIP	2022, R, L
13212−7427	HDS1874	0.″1 HIP	2021−22, R, B, L
13297−4611	HDS1890	0.″1 HIP	2018, R, B, L
13366−6433	HDS1909	0.″1 HIP	2022, L
13400−7047	HDS1918	0.″1 HIP	2018, R, L
14029−3511	I 1574	0.″2 Vis 1927	2017−22, R, B
14141+1258	CHR 41	0.″2 Sp 1984	2014, R, B
14157+1911	HDS2003	0.″1 HIP	2019, S
14598−2201	TOK 47Aa,Ab	0.″04 Sp 2009	2013−17, R, S
15073+1827	A 2385AB	0.″1 Vis 1910	2018−21, R, B, S
15172−3435	BRR 10Ba,Bb	0.″7 AO 1994	2022, R, B, L
15210−1522	MCA 41	0.″4 Sp 1980	2008−14, R, L
15355−1447	WRH 20Aa,Ab	0.″1 Vis 1937	2009−23, S
15462−2804	CHR 50Aa,Ab	0.″2 Sp 1983	2009−22, S
16102−4008	I 1082AB	0.″4 Vis 1912	2008−22, R, B, L
16133+1332	CHR 52Aa,Ab	0.″2 Sp 1983	2008−09, R, S
16142−5047	TOK 409	0.″1 Sp 2014	2015−22, R, B, S, V
16406+0413	CHR 56Aa,Ab	0.″1 Sp 1985	2014−22, R, B, V
16438−5330	CHR 147Aa,Ab	0.″04 Sp 1989	2008−14
16542−4150	CHR 252Aa,Ab	0.″1 Sp 1994	2009−19, R, L
16593−1926	HDS2403	0.″4 HIP	2018, L, R
17376−1524	ISO 6Aa,Ab	0.″3 Sp 1987	2023, B
17449−5733	HLN 44Aa,Ab	0.″2 Vis 1967	2008−19, R, B
18073+0934	STT 342Aa,Ab	1.″3 Vis 1842	2023, B
18218−1619	CHR 69	0.″1 Sp 1985	2013−18, R, L
18237+2146	TOK 60Aa,Ab	0.″04 Sp 2009	2018−21, B, V, L
18367+0640	CHR 76Aa,Ab	0.″1 Sp 1985	2008−09, R, B, S
18448−2501	CHR 78	0.″1 Sp 1983	2014−19, R, V
18582+1722	CHR 82Aa,Ab	0.″2 Sp 1984	2015, R, L
19098−2101	FIN 311AB	0.″1 Vis 1936	2009−18
19098−2101	FIN 311AC	0.″4 Vis 1936	2009−18
19247+0833	WSI 108	0.″1 Sp 2008	2015−21, R, B, S
19255+0307	BNU 6Aa,Ab	0.″1 Sp 1979	2023, S
19298−1102	HDS2771	0.″1 HIP	2015−21, R, B
19409−0152	TOK 424	0.″04 Sp 2014	2015−21
20011+0931	CHR 118	0.″2 Sp 1985	2018, R, L

[a] Additional indications of the spurious nature of resolutions: R – no excess noise in Gaia DR3, RUWE<2; L – long estimated period; B – no significant PM anomaly in (Brandt 2021); S – short estimated period or spectroscopic coverage; V – artefact caused by SOAR vibration.

3.4.1. *Notes to Individual Spurious Pairs*

15073+1827 = A 2358AB : This system is another classic "ghost" binary Tokovinin (2012), with many measures and an orbit Eggen (1946), but many unresolved measures and other indications confirming its spurious nature.

18582+1722 = CHR 82Aa,Ab : The orbit of Benedict et al. (2007), previously assigned to this pair is obviously the much closer pair CIA 14Aa1,2 of Gallenne et al. (2019).

19255+0307 = BNU 6Aa,Ab : The ESA (1997) orbit is of the unresolved pair associated with the Kamper et al. (1989) orbit and not the never confirmed wider speckle pair of Bonneau et al. (1980).

4. SUMMARY AND OUTLOOK

The program continues to investigate the multiplicity of various stellar samples, the kinematics and dynamics of binary and hierarchical systems, to find new pairs, and to obtain orbital solutions for them as quickly thereafter as possible. Investigation of close pairs have found many that are rapidly moving and others which are anomalous detections and can henceforward be ignored. For those which are rapidly moving, ascertaining the proper observing cadence can be challenging, but we have identified, when possible, specific future instances when observations are needed.

We thank the SOAR operators for efficient support of this programand the SOAR director J. Elias for allocating some technical time. This work is based in part on observations carried out under CNTAC programs CN2019A-2, CN2019B-13, CN2020A-19, CN2020B-10and CN2021B-17. R.A.M. and E.C. acknowledge support from the FONDECYT/CONICYT grant #1190038. The research of A.T. is supported by the NSFs NOIRLab.

This work used the SIMBAD service operated by Centre des Données Stellaires (Strasbourg, France), bibliographic references from the Astrophysics Data System maintained by SAO/NASAand the Washington Double Star Catalog maintained at the USNO. This work has made use of data from the European Space Agency (ESA) mission Gaia (https://www.cosmos.esa.int/gaia) processed by the Gaia Data Processing and Analysis Consortium (DPAC, https://www.cosmos.esa.int/web/gaia/dpac/consortium). Funding for the DPAC has been provided by national institutions, in particular the institutions participating in the Gaia Multilateral Agreement.

Facility: SOAR

REFERENCES

Aitken, R.G. 1964, The Binary Stars (New York: Dover), 110

Anguita-Aguero, J., Mendez, R., Claveria, R. M. & Costa, E. 2022, AJ 163, 118

Argue, A.N., Hebden, J.C., Morgan, B.L. et al. 1985, MNRAS 216, 447

Batten, A.H., Fletcher, J.M., Hill, G., Wenxian, Lu & Morbey, C.L. 1991, PASP 103, 294

Benedict, G.F., McArthur, B.E., Feast, M.W., Barnes, T.G., Harrison, T.E., Patterson, R.J., Menzies, J.W., Bean, J.L. & Freedman, W.L. 2007, AJ 133, 1810

Blunt, S., Wang, J., Angelo, I. et al. 2020, AJ 159, 89

Bonavita, M., Gratton, R., Desidera, S. et al. 2021, ArXiv preprint 2103.13706

Bonneau, D., Blazit, A., Foy, R. & Labeyrie, A. 1980, A&AS 42, 185

Brandt, T. D. 2021, ApJS 254, 42

Brandt, T. D., Dupuy, T. J., Li, Y. et al. 2021, AJ 162, 186

Colacevic, A. 1941, Oss. e Mem. Arcetri 59, 15

Cortes-Contreras, M., Bejar, V. J. S., Caballero, J. A. et al. 2017, A&A 597, 47

Duquennoy, A., Mayor, M. & Halbwachs, J.-L. 1991, A&AS 88, 281

Eggen, O.J. 1946, AJ 52, 81

El-Badry, K., Rix, H.-W. & Heintz, T.M. 2021, MNRAS 506, 2269

The Hipparcos and Tycho Catalogues (ESA SP-1200) (Noordwijk: ESA) [DMSA/O Orbital Solutions]

Gaia Collaboration et al. 2018, A&A, 616A, 1

Gaia Collaboration, Brown, A. G. A., Vallenari, A., et al. 2021, A&A 649, A1 (Gaia EDR3)

Gallenne, A., Kervella, P., Borgniet, S., Merand, A., Pietrzynski, G., Gieren, W., Monnier, J.D., Schaefer, G.H., Evans, N.R., Anderson,R.I., Baron, F., Roettenbacher, R.M. & Karczmarek, P. 2019, A&A 622A, 164

Gómez, J., Docobo, J. A., Campo, P., Andrade, M., Mendez, R. & Costa, E. 2022, MNRAS 509, 4229

Harris, D.L., III, Strand, K.Aa. & Worley, C.E. 1963, in Stars and Stellar Systems, Vol. 3, Basic Astronomical Data, ed. K.
A. Strand (Chicago: Univ. Chicago Press), 273

Hartkopf, W.I., McAlister, H.A. & Franz, O.G. 1989, AJ 98, 1014

Hartkopf, W.I., Mason, B.D. & Worley, C.E. 2001, AJ 122, 3472 (ORB6)

Hartkopf, W.I., Tokovinin, A. & Mason, B.D. 2012, AJ 143, 42

Hirsch, L.A., Rosenthal, L., Fulton, B.J. et al. 2021, AJ 161, 134

Horch, E.P., van Belle, G.T., Davidson, J.W., Jr. et al. 2015, AJ 150, 151

Horch, E.P., Casetti-Dinescu, D.I., Camarata, M.A. et al. 2017, AJ 153, 212

Horch, E.I., Tokovinin, A., Weiss, S.A. et al. 2019, AJ 157, 56

Horch, E.P., Broderick, K.G., Casetti-Dinescu, D.I. et al. 2021, AJ 161, 295

Isobe, S. 1991, Proc. Astron. Soc. Australia 9, 270

Izmailov, I.S. 2019, AstL 45, 30

Kamper, K.W., Legget, D. & McCarthy, D.W. 1989, AJ 98, 686

Kenyon, S., Lawrence, J.S., Ashley, M. et al. 2006, PASP 118, 924

Mann, A.W., Dupuy, T., Kraus, A. et al. 2019, ApJ 871, 63

Mason, B.D., Wycoff, G.L., Hartkopf, W.I. et al. 2001, AJ 122, 3466 (WDS)

McAlister, H.A., Mason, B.D., Hartkopf, W.I. & Shara, M.M. 1993, AJ 106, 1639

Mendez, R.A., Clavería, R.M., Orchard, M.E. & Silva, J.F. 2017, AJ 154, 187

Mendez, R.A., Clavería, R.M. & Costa, E. 2021, AJ 161, 155

Ruane, G., Ngo, H., Mawet, D. et al. 2019, AJ 157, 118

Tokovinin, A. 2012, AJ 144, 56

Tokovinin, A. 2016a, AJ 152, 138

Tokovinin, A. 2016b, Orbit: IDL Software For Visual, Spectroscopic, And Combined Orbits, Zenodo, doi: 10.5281/zenodo.61119

Tokovinin, A. 2017, AJ 154, 110

Tokovinin, A. 2018, PASP 130, 5002

Tokovinin, A. 2021a, AJ 161, 144

Tokovinin, A. 2021b, Universe 7(9), 352

Tokovinin, A. 2022, AJ 163, 127

Tokovinin, A. 2023, AJ 165, 165

Tokovinin, A. 2023, AJ 165, 180

Tokovinin, A. & Briceño, C. 2020, AJ 159, 15

Tokovinin, A. Cantarutti, R., Tighe, R. et al. 2010b, PASP 122, 1483

Tokovinin, A. & Latham, D.W. 2020, AJ 160, 251

Tokovinin, A., Mason, B.D. & Hartkopf, W.I. 2010a, AJ 139, 743 (TMH10)

Tokovinin, A., Mason, B.D. & Hartkopf, W.I. 2014, AJ 147, 123

Tokovinin, A., Mason, B.D., Hartkopf, W.I. et al. 2015, AJ 150, 50

Tokovinin, A., Mason, B.D., Hartkopf, W.I. et al. 2016, AJ 152, 116

Tokovinin, A., Mason, B.D., Hartkopf, W.I. et al. 2018, AJ 155, 235

Tokovinin, A., Mason, B.D., Mendez, R.A. et al. 2019, AJ 158, 148

Tokovinin, A., Mason, B.D., Mendez, R.A. et al. 2020, AJ 160, 7

Tokovinin, A., Mason, B.D., Mendez, R.A., Costa, E., Mann, A.W. & Henry, T.J. 2021, AJ 162, 41

Tokovinin, A., Mason, B.D., Mendez, R.A. & Costa, E. 2022, AJ 164, 58

van den Bos, W.H. 1928, Ann. Leiden Obs. 14, Pt. 4

van Leeuwen, F. 2007, A&A 474, 653

Vrijmoet, E.H., Tokovinin, A., Henry, T.J. et al. 2022, AJ 163, 178

White, G.L., Jauncey, D.L., Reynolds, J.E. et al. 1991, MNRAS 248, 411

Worley, C.E. & Behall, A.L. 1973, AJ 78, 650

Ziegler, C., Tokovinin, A., Briceño, C. et al. 2020, AJ 159, 19

Ziegler, C., Tokovinin, A., Latiolais, M., Briceño, C., Law, N. & Mann, A.W. 2021, AJ 162, 192

Table 5. Reliable Orbital Elements

WDS Desig. α, δ (2000)	Discoverer Designation	P (yr)	a ($''$)	i ($^\circ$)	Ω ($^\circ$)	T_0 (yr)	e	ω ($^\circ$)	Reference	Gr	Notes?
00160−4816	TOK 808	6.98	0.14759	23.0	211.8	2023.388	0.3214	20.4	Tok2023a	3	
		±0.12	±0.00063	±1.6	±5.8	±0.024	±0.0058	±8.7			
00261−1123	YR 4	39.12	0.2727	150.3	81.0	2025.44	0.694	66.	Tok2023a	3	
		0.75	0.0026	5.2	8.7	0.21	0.016	11.			
00324+0657	MCA 1Aa,Ab	27.503	0.1594	110.7	105.80	1989.00	0.810	14.4	Msn2021c	2	
		0.052	0.0022	2.3	0.74	0.10	0.024	2.2			
01104−6727	GKI 3	1.14451	0.12478	126.44	89.55	2013.4206	0.1624	39.3	Kpp2020f	1	
		0.00022	0.00060	0.47	0.60	0.0057	0.0030	2.1			
01388−1758	LDS 838	26.351	2.0220	128.78	146.22	2024.855	0.6143	284.27	MnA2019	2	⋆
		0.049	0.0042	0.52	0.43	0.034	0.0034	0.81			
01559+0151	STF 186	167.7	1.048	74.6	220.07	1893.8	0.717	44.3	Msn2021c	2	
		3.1	0.035	2.4	0.65	3.1	0.057	3.5			
02290−1959	RST2280Aa,Ab	31.50	0.5290	163.5	168.3	2020.764	0.6497	18.3	Tok2023a	3	
		0.49	0.0070	1.7	5.2	0.012	0.0039	5.2			
02418−5300	SYU 4Ba,Bb	4.946	0.06887	138.7	139.7	2021.179	0.4597	276.0	Tok2023a	2	
		0.022	0.00075	1.4	2.3	0.019	0.0093	3.0			
02424+2001	BLA 1Aa,Ab	8.868	0.05467	71.50	101.07	1981.133	0.3767	96.0	Msn1997a	1	
		0.016	0.00067	0.62	0.75	0.089	0.0087	3.4			
02434−6643	FIN 333	35.19	0.269	92.20	33.99	1997.15	0.863	344.2	Msn2011a	3	
		0.16	0.010	0.78	0.24	0.53	0.068	7.0			
03125+1857	HDS 408	9.525	0.0583	121.3	155.0	2023.72	0.844	329.	Cve2017b	3	
		0.058	0.0020	9.6	4.9	0.19	0.058	10.			
03271+1845	CHR 10AB	8.408	0.0569	25.7	190.	2022.81	0.586	85.	Tok2020e	2	
		0.025	0.0018	9.0	26.	0.17	0.031	31.			
03311−0029	HDS 444	20.41	0.0783	37.1	49.6	2025.02	0.581	338.	Tok2023a	3	
		0.90	0.0020	3.1	7.6	0.21	0.038	11.			
03544−4021	FIN 344AB	14.077	0.06147	31.50	65.5	2008.058	0.5847	51.2	Tok2015c	2	
		0.015	0.00027	0.88	1.8	0.022	0.0030	2.2			
04108−4200	HDS 530	23.80	0.224	110.6	193.0	2018.95	0.582	284.3	Tok2023a	3	
		0.74	0.013	2.5	1.6	0.18	0.014	3.5			
04119+2338	CHR 14Aa,Ab	43.41	0.4200	77.5	156.1	1993.31	0.924	258.7	Msn2010a	3	
		0.80	0.0070	3.1	1.6	0.39	0.028	7.7			
04312+0157	HDS 585	74.78	0.3941	76.68	80.40	2013.975	0.4705	346.33	Tok2019c	3	

Table 5 *continued*

Table 5 *(continued)*

WDS Desig. α, δ (2000)	Discoverer Designation	P (yr)	a ($''$)	i ($^\circ$)	Ω ($^\circ$)	T_0 (yr)	e	ω ($^\circ$)	Reference	Gr	Notes?
		0.28	0.0020	0.15	0.25	0.069	0.0023	0.46			
04330−1633	CRI 7Ba,Bb	5.685	0.0887	98.48	171.07	2017.39	0.1969	77.4	Tok2023a	3	
		0.039	0.0018	0.45	0.90	0.17	0.0057	9.2			
04400−3105	HDS 602	28.01	0.3112	118.10	174.47	2021.796	0.6963	81.51	Tok2019c	3	
		0.20	0.0019	0.40	0.40	0.019	0.0015	0.92			
04590−1623	BU 314AB	54.98	0.4783	119.0	129.20	2033.84	0.927	334.7	Doc2019e	2	
		0.10	0.0042	4.2	0.61	0.12	0.017	1.3			
05174−3522	TSN 1	0.71094	0.05853	107.94	164.26	2022.3670	0.2242	140.7	Tok2023a	2	
		0.00038	0.00042	0.39	0.55	0.0056	0.0041	3.0			
05429−0648	A 494AB	20.1843	0.20976	72.15	96.52	1959.954	0.39553	273.97	Msn2009	2	
		0.0062	0.00072	0.11	0.18	0.028	0.00097	0.45			
05525−0217	HDS 787	11.851	0.1200	56.90	153.3	1999.917	0.2285	91.8	Tok2017b	2	
		0.023	0.0015	0.66	1.1	0.067	0.0034	2.5			
06035+1941	MCA 24	13.021	0.0512	111.4	227.4	2006.64	0.806	296.6	Tok2020e	2	
		0.029	0.0016	6.3	2.5	0.11	0.045	6.9			
06159+0110	RST5225	29.551	0.16583	13.7	185.6	1995.128	0.3773	197.	Msn2009	2	
		0.037	0.00078	1.9	9.9	0.060	0.0035	10.			
06214+0216	A 2667	96.5	0.4243	62.85	110.30	1933.1	0.4225	252.0	Msn2009	2	
		1.7	0.0018	0.47	0.20	1.8	0.0047	2.1			
06237−3319	TOK 823Aa,Ab	5.013	0.04626	129.9	199.4	2022.060	0.6601	327.3	Tok2022g	3	
		0.031	0.00028	1.3	1.0	0.013	0.0081	1.8			
06510+0551	HDS 950	29.11	0.1205	98.02	162.3	2016.79	0.3977	270.7	Tok2019c	3	
		0.23	0.0047	0.68	1.3	0.36	0.0050	5.4			
07043−0303	A 519AB	43.84	0.2765	98.85	96.28	2007.446	0.559	0.49	Tok2015c	2	
		0.34	0.0025	0.44	0.12	0.093	0.011	0.75			
07508+0317	A 2880	109.6	0.1815	47.86	93.32	1991.903	0.6046	291.23	Hrt2000a	2	
		2.1	0.0022	0.45	0.57	0.065	0.0055	0.66			
07548−6613	TOK 830	7.46	0.05329	147.9	114.8	2021.638	0.4088	98.6	Tok2022g	3	
		0.15	0.00097	1.5	2.9	0.016	0.0099	3.1			
08280−3507	FIN 314Aa,Ab	35.41	0.07833	38.8	289.	2005.25	0.9279	297.	Tok2018e	3	
		0.19	0.00046	4.8	12.	0.39	0.0090	16.			
08539+0149	A 2554	44.43	0.2102	161.4	311.8	2021.750	0.4859	0.8	Tok2015c	2	
		0.19	0.0011	2.1	5.8	0.064	0.0053	6.3			
08589+0829	DEL 2	5.5340	0.3925	123.1	279.89	2006.434	0.7723	19.9	Tok2015c	2	

Table 5 *continued*

Table 5 *(continued)*

WDS Desig. α, δ (2000)	Discoverer Designation	P (yr)	a ($''$)	i ($^\circ$)	Ω ($^\circ$)	T_0 (yr)	e	ω ($^\circ$)	Reference	Gr	Notes?
		0.0036	0.0019	1.2	0.60	0.39	0.0082	1.2			
09125−4032	B 1115	135.49	0.33052	141.98	104.37	2005.782	0.4413	271.57	Tok2014a	3	
		0.60	0.00072	0.16	0.47	0.025	0.0018	0.36			
09156−1036	MTG 2	5.0419	0.1992	116.23	112.81	2014.191	0.4760	273.0	Msn2021a	2	
		0.0023	0.0010	0.59	0.52	0.015	0.0045	1.3			
09243−3926	FIN 348	41.58	0.12249	160.5	91.3	2004.920	0.4589	336.0	Tok2021f	2	
		0.19	0.00047	2.1	2.7	0.095	0.0065	3.0			
09307−4028	COP 1	34.11	0.8110	58.45	288.24	2004.062	0.4375	47.76	Msn2021a	1	
		0.12	0.0017	0.15	0.13	0.035	0.0030	0.53			
09442−2746	FIN 326	18.423	0.10904	126.19	175.66	2020.913	0.4956	138.04	Tok2020e	1	
		0.019	0.00032	0.44	0.44	0.025	0.0031	0.86			
10112−3245	HDS1469	18.68	0.1076	121.6	255.2	2018.22	0.407	343.8	Tok2016e	3	⋆
		1.04	0.0069	2.4	3.8	0.15	0.030	4.1			
10214−2616	HDS1491	22.14	0.11934	150.1	250.79	2024.09	0.1954	1.1	Tok2019c	3	
		0.28	0.00038	1.0	0.92	0.11	0.0036	3.5			
10282−2548	FIN 308AB	32.57	0.1442	48.2	157.8	2018.157	0.7375	269.3	Tok2015c	2	
		0.11	0.0019	1.2	1.9	0.076	0.0051	2.8			
10430−0913	WSI 112	27.62	0.577	121.0	282.6	2002.11	0.440	284.1	Tok2022g	3	
		0.24	0.012	2.7	1.1	0.11	0.024	3.1			
11272−1539	HU 462	48.16	0.4579	169.0	135.	1960.9	0.091	1.	Msn2021c	2	
		0.75	0.0056	4.9	18.	1.1	0.012	14.			
11436−1401	YSC 210	17.899	0.16328	117.81	207.83	2008.808	0.1684	134.9	Tok2023a	3	
		0.031	0.00034	0.14	0.23	0.056	0.0017	1.2			
12290+0826	WSI 113	11.6373	0.3088	108.43	188.87	2008.206	0.29482	89.00	AST2016	2	
		0.0052	0.0016	0.14	0.35	0.022	0.00077	0.79			
13123−5955	SEE 170AB	27.51	0.16644	60.22	279.8	2022.140	0.6657	18.3	Doc2021d	2	
		0.42	0.00093	0.96	1.0	0.071	0.0084	2.8			
13217−3919	HDS1875	40.72	0.2024	119.83	195.1	2019.518	0.5250	230.73	Tok2020g	3	
		0.77	0.0031	0.66	1.7	0.091	0.0062	0.94			
13574−6229	FIN 370	18.757	0.13544	144.34	269.32	2005.849	0.2193	359.81	Mdz2021	2	
		0.017	0.00026	0.33	0.48	0.023	0.0020	0.77			
14275−3527	TOK 724	4.103	0.0381	89.40	317.62	2018.499	0.480	31.3	Tok2022g	2	
		0.020	0.0011	0.67	0.60	0.054	0.037	5.1			
14462−2111	FIN 309	12.9212	0.18189	28.24	287.0	1995.265	0.6373	34.6	Msn2010c	1	

Table 5 *continued*

Table 5 *(continued)*

WDS Desig. α, δ (2000)	Discoverer Designation	P (yr)	a ($''$)	i ($^\circ$)	Ω ($^\circ$)	T_0 (yr)	e	ω ($^\circ$)	Reference	Gr	Notes?
		0.0065	0.00051	0.74	2.0	0.019	0.0022	2.4			
14567−6247	FIN 372	38.20	0.08808	146.8	223.8	1993.76	0.2775	64.7	Msn2010c	2	
		0.20	0.00073	1.8	3.0	0.24	0.0080	4.9			
14589+0636	WSI 81	5.4589	0.09533	154.3	44.7	2016.653	0.4059	328.5	Tok2018e	2	
		0.0052	0.00041	1.1	2.7	0.012	0.0030	3.2			
15122−1948	B 2351Aa,Ab	23.512	0.12932	154.2	173.8	1971.034	0.2440	340.1	Msn2021c	1	
		0.026	0.00064	1.0	2.3	0.076	0.0029	2.8			
15537−0429	TOK 725	11.26	0.08241	166.6	198.	2020.729	0.5685	334.	Tok2021f	3	
		0.13	0.00064	4.5	20.	0.027	0.0081	20.			
16430−0857	YSC 155	10.772	0.0655	118.0	149.1	2021.631	0.738	12.8	Tok2021f	2	
		0.081	0.0011	3.4	2.1	0.087	0.029	5.2			
16555−0820	KUI 75AB	1.71741	0.22949	161.30	164.7	1991.6311	0.04225	128.7	Sod1999	1	⋆
		0.00005	0.00046	0.49	1.6	0.0063	0.00092	2.3			
17077+0722	YSC 62	14.327	0.30649	113.09	241.44	2006.535	0.4889	23.57	Mdz2021	2	
		0.025	0.00094	0.34	0.27	0.028	0.0034	0.79			
17119−0151	LPM 629	34.484	0.7688	19.94	143.9	1988.130	0.1969	218.7	Doc2018l	3	
		0.029	0.0021	0.88	4.4	0.057	0.0034	4.6			
17151−2750	ELP 40	19.789	0.11741	141.8	39.4	2009.20	0.2392	11.8	Tok2022g	3	
		0.086	0.00084	1.6	1.4	0.12	0.0084	3.3			
17190−3459	MLO 4AB	42.152	1.8260	127.662	133.574	1933.752	0.57374	68.451	Izm2019	1	⋆
		0.039	0.0017	0.034	0.063	0.079	0.00029	0.056			
17304−0104	STF2173AB	46.707	0.9693	98.76	151.623	2008.55	0.1784	324.53	Hei1994a	1	⋆
		0.069	0.0018	0.11	0.098	0.11	0.0022	0.94			
19167−4553	RST4036	7.6834	0.24586	124.499	200.172	1995.043	0.26067	240.72	Msn2019	1	
		0.0052	0.00018	0.066	0.097	0.016	0.00064	0.24			
21044−1951	FIN 328	27.896	0.2639	163.7	160.4	2002.41	0.4087	47.	Doc2013d	2	
		0.032	0.0016	3.4	9.8	0.13	0.0068	11.			
21214+1020	A 617	6.0570	0.0969	132.4	281.1	1991.855	0.827	13.2	Sod1999	1	
		0.0019	0.0011	4.4	2.1	0.023	0.020	3.3			
21274−0701	HDS3053	20.633	0.16476	50.27	152.93	2015.756	0.3545	149.3	Mit2021	2	
		0.051	0.00066	0.40	0.52	0.044	0.0027	1.1			
22508−6543	HDS3246	20.390	0.2110	94.01	92.50	2016.327	0.4202	326.1	Tok2018e	3	
		0.070	0.0011	0.15	0.20	0.054	0.0019	1.3			
22532−3750	HDS3250Aa,Ab	12.91	0.1261	42.5	42.5	2012.00	0.086	322.	Tok2020e	3	

Table 5 *continued*

Table 5 *(continued)*

WDS Desig. α, δ (2000)	Discoverer Designation	P (yr)	a (″)	i (°)	Ω (°)	T_0 (yr)	e	ω (°)	Reference	Gr	Notes?
		0.47	0.0048	3.0	4.8	0.48	0.030	18.			
23191−1328	MCA 74Aa,Ab	6.3211	0.1912	46.8	158.7	2012.405	0.1735	37.1	Doc2018f	1	
		0.0041	0.0023	1.2	1.8	0.058	0.0062	4.3			

Table 6. Provisional Orbital Elements

WDS Desig. α, δ (2000)	Discoverer Designation	P (yr)	a (″)	i (°)	Ω (°)	T_0 (yr)	e	ω (°)	Reference	Gr	Notes?
00003−4417	I 1477	119.1	0.424	60.8	148.7	2012.9	0.710	299.	Cve2010e	3	
00164−7024	HEI 198	52.4	0.1122	144.9	176.3	2012.33	0.483	238.	Tok2017b	3	
02514−2139	DON 43	121.2	0.2068	41.5	209.	1976.0	0.399	283.	Doc2016i	3	
03526−0829	RST4762AB	151.4	0.1668	120.1	264.8	1994.0	0.264	327.	Tok2023a	3	
05033−2315	BEU 7	15.34	0.326	136.3	273.	2022.2	0.093	75.	Tok2023a	4	
05320−0018	HEI 42Aa,Ab	317.4	0.355	107.3	142.8	1960.2	0.6750	257.	Tok2014a	4	
06337−2853	B 700	200.5	0.219	114.7	145.9	2008.7	0.826	133.	Tok2023a	4	
06354−0403	JNN 271	10.4	0.2017	88.42	171.47	2022.6	0.263	9.	Tok2023a	4	
07175−4659	I 7	85.9	1.05	104.	242.2	1958.4	0.976	251.	Tok2015c	3	
07185−5721	HDS1013Aa,Ab	56.6	0.3511	20.	171.	1997.9	0.216	124.	Hrt2012a	3	
07417+0942	STF1130	902.9	1.776	51.7	327.6	1981.2	0.793	346.5	Msn1999a	4	
07522−4035	TOK 195	7.149	0.0611	82.9	272.24	2012.13	0.385	350.	Tok2015c	3	
08085−5237	B 1586	201.8	0.314	74.42	86.1	2018.94	0.8476	297.0	Tok2022g	4	
08369−7857	KOH 79AB	56.2	0.1953	108.5	181.17	1991.6	0.1786	279.	Tok2016e	3	
08486+0237	A 2551	73.7	0.1484	36.8	160.2	1951.1	0.663	70.	Msn2017g	3	
10283−2416	TOK 537Aa,Ab	31.2	0.336	55.11	157.10	2021.825	0.694	10.7	Tok2021f	4	
10595−4130	RST2720	217.2	0.210	31.	241.	1975.4	0.241	53.	Tok2023a	4	
11128−7402	B 2009	142.0	0.276	140.	290.	1971.4	0.241	295.	Tok2023a	4	
11192−1950	TOK 383Aa,Ab	12.67	0.0429	134.9	177.0	2020.09	0.380	328.	Tok2020g	3	
11431−3601	I 1546	149.6	0.2017	121.3	272.9	2000.6	0.137	286.	Tok2022g	4	
12096−6727	HDS1716	56.2	0.150	53.6	57.6	2019.08	0.503	351.2	Tok2019c	3	
12117−5222	RIZ 2	3.626	0.0440	164.	225.	2019.237	0.619	54.	Tok2023a	3	
12228−0405	BWL 29AB	9.783	0.234	103.8	210.2	2023.56	0.741	252.	Tok2023a	4	
12446−5717	FIN 65AB	111.6	0.292	112.1	242.7	1946.1	0.413	114.	Doc2013d	3	
13344−5931	TOK 403	17.03	0.1423	117.53	252.65	2021.090	0.4587	90.3	Tok2020e	3	
13535+1257	BEU 18	7.4020	0.18275	127.31	187.62	2023.701	0.5207	355.5	Tok2022g	2	⋆
14516−4335	FIN 319	10.874	0.0853	30.8	118.0	2020.650	0.8013	344.2	Doc2020d	2	⋆
15251−2340	RST2957	57.21	0.21689	85.59	93.019	2027.57	0.5505	338.4	Tok2016e	3	
15273+0942	A 1120	51.8	0.174	67.0	156.2	1931.4	0.723	340.	Msn2014b	3	
15394−1355	HDS2210	41.12	0.1701	109.4	172.34	2014.8	0.054	11.	Tok2018e	3	
15433−0515	TOK 594Aa,Ab	3.809	0.0561	57.5	142.2	2019.053	0.791	137.2	Tok2021f	3	
15440+0231	RDR 6Ba,Bb	2.9726	0.1267	126.	190.5	2022.868	0.939	331.7	Tok2021b	2	⋆
15462−2804	KOH 49Ca,Cb	18.811	0.11663	136.55	280.7	2038.514	0.3114	35.54	Tok2021c	2	⋆
16016−7843	HDS2259	62.9	0.361	88.2	156.46	2004.30	0.801	45.	Tok2023a	4	
16038+1406	HDS2265	50.2	0.335	59.0	178.1	2021.16	0.840	343.	Tok2020e	4	
16271−1205	HU 158	234.3	0.297	107.9	315.1	2000.1	0.682	358.2	Tok2022g	4	
16514−2450	B 2397	69.6	0.1578	119.0	201.2	2020.4	0.067	250.	Tok2019c	3	

Table 6 *continued*

Table 6 *(continued)*

WDS Desig. α, δ (2000)	Discoverer Designation	P (yr)	a ($''$)	i ($^\circ$)	Ω ($^\circ$)	T_0 (yr)	e	ω ($^\circ$)	Reference	Gr	Notes?
16573−5344	SYU 11Aa,Ab	9.104	0.08702	6.6	174.	2023.934	0.5708	333.	Tok2022g	3	
17207−0706	A 2593AB	75.5	0.2589	128.9	167.6	1986.9	0.094	48.	Msn2014a	3	
17375−3747	B 915AB	128.4	0.278	65.2	314.2	2147.0	0.052	25.	Msn2017a	4	
17387−2155	HDS2492	21.48	0.1027	26.9	220.	2006.47	0.392	15.	Tok2023a	3	
17460−3435	HDS2510AB	41.5	0.134	64.3	241.4	2012.1	0.298	304.	Tok2022g	3	
18281−2645	HDS2615AB	37.29	0.557	95.6	173.23	1988.66	0.794	84.5	Tok2015c	3	
19474−0148	A 2993AB	64.1	0.1396	130.1	174.4	2026.92	0.6880	46.0	Hrt2014b	3	
20073−5127	RST1059	161.7	0.1697	17.8	259.	2014.5	0.275	315.	Mdz2017	3	
23209+1643	HEI 88	34.09	0.16872	25.2	120.2	2002.97	0.6365	268.1	Cve2011a	3	
23218−1217	HU 95	162.2	0.3994	155.	202.	1943.2	0.374	113.	Msn1999c	4	
23286−3821	HDS3342	47.7	0.1175	129.5	305.7	2014.9	0.359	337.1	Tok2019c	3	
23455−1610	MTG 5	21.46	0.4192	98.65	9.13	2024.373	0.4761	352.7	Tok2023a	3	